# Bidirectional Mendelian Randomization Highlights Causal Relationships Between Circulating INHBC and Multiple Cardiometabolic Diseases and Traits

Nellie Y. Loh,[1] Daniel B. Rosoff,[1,2,3] Rebecca Richmond,[1,3] Raymond Noordam,[4] George Davey Smith,[3] David Ray,[1,5] Fredrik Karpe,[1,5] Falk W. Lohoff,[2] and Constantinos Christodoulides[1,5]

*Diabetes 2024;73:2084–2094 | https://doi.org/10.2337/db24-0168*



**Human genetic and transgenic mouse studies have highlighted a potential liver-adipose tissue endocrine axis, involving activin C (Act-C) and/or Act-E and ALK7, influencing fat distribution and systemic metabolism. We investigated the bidirectional effects between circulating INHBC, which homodimerizes into Act-C, and adiposity traits, insulin resistance, inflammation, and cardiometabolic disease risk. Additionally, we examined whether Act-C is an ALK7 ligand in human adipocytes. We used Mendelian randomization and in vitro studies in immortalized human abdominal and gluteal adipocytes. Circulating INHBC was causally linked to reduced lower-body fat, dyslipidemia, and increased risks of coronary artery disease (CAD) and nonalcoholic fatty liver disease (NAFLD). Conversely, upper-body fat distribution, obesity, hypertriglyceridemia, subclinical inflammation, and type 2 diabetes positively impacted plasma INHBC levels. Mechanistically, an atherogenic lipid profile may partly explain the INHBC-CAD link, while inflammation and hypertriglyceridemia may partly explain how adiposity traits affect circulating INHBC. Phenome-wide Mendelian randomization showed weak causal relationships between higher plasma INHBC and impaired kidney function and higher gout risk. In human adipocytes, recombinant Act-C activated SMAD2/3 signaling via ALK7 and suppressed lipolysis. In summary, INHBC influences systemic metabolism by activating ALK7 in adipose tissue and may serve as a drug target for atherogenic dyslipidemia, CAD, and NAFLD.**

## ARTICLE HIGHLIGHTS

- We explored the bidirectional relationships between circulating INHBC and cardiometabolic traits and diseases, and investigated whether activin C, an INHBC homodimer, acts as an ALK7 ligand in human adipocytes.
- Elevated circulating INHBC was linked to dyslipidemia, increased coronary artery disease, and nonalcoholic fatty liver disease risk. Conversely, upper-body obesity, hypertriglyceridemia, inflammation, and diabetes increased circulating INHBC, potentially creating a vicious cycle. Activin C activated ALK7 signaling in adipocytes and suppressed lipolysis.
- INHBC is a novel hepatokine influencing systemic metabolism and a potential drug target for cardiometabolic diseases.

Subcutaneous white adipose tissue (WAT) possesses a unique ability to safely store surplus calories as triglycerides (TAG). Reduced subcutaneous WAT storage capacity, often seen in obesity or upper-body fat distribution, can lead to ectopic lipid buildup in muscle and liver, causing lipotoxicity. This triggers insulin resistance, systemic inflammation, and an increased risk of type 2 diabetes, coronary artery disease (CAD), and nonalcoholic fatty liver disease (NAFLD) (1,2).

[1]Oxford Centre for Diabetes, Endocrinology and Metabolism, Radcliffe Department of Medicine, University of Oxford, Oxford, U.K.
[2]National Institute on Alcohol Abuse and Alcoholism, National Institutes of Health, Bethesda, MD
[3]MRC Integrative Epidemiology Unit, University of Bristol, Bristol, U.K.
[4]Department of Internal Medicine, Section of Gerontology and Geriatrics, Leiden University Medical Center, Leiden, the Netherlands
[5]NIHR Oxford Biomedical Research Centre, John Radcliffe Hospital, Oxford, U.K.

Corresponding author: Constantinos Christodoulides, costas.christodoulides@ocdem.ox.ac.uk

Received 29 February 2024 and accepted 5 September 2024

This article contains supplementary material online at https://doi.org/10.2337/figshare.26997682.

N.Y.L. and D.B.R. contributed equally to this work.

The cellular and molecular mechanisms regulating subcutaneous WAT fat storage capacity are poorly understood. Discovering genetic variants that influence WAT lipid storage potential and protect against disease can uncover new disease mechanisms and treatment targets. For example, the discovery of loss-of-function (LoF) *PCSK9* variants linked with lower LDL-cholesterol and protection from CAD led to novel CAD therapies (3–5).

The transforming growth factor β (TGFβ) superfamily is crucial for WAT development, function, and metabolic homeostasis (6–9). Activin receptor-like kinase 7 (ALK7), encoded by *ACVR1C*, is one of seven type I TGFβ superfamily receptors. In humans, *ACVR1C* is most highly expressed in WAT (https://www.gtexportal.org) and *ACVR1C* LoF variants are associated with lower BMI-adjusted waist-to-hip ratio (WHRadjBMI), a surrogate of visceral versus gluteofemoral adiposity, and protection from type 2 diabetes (10–13). Pharmacologic inhibition of ALK7 signaling also seems tractable, since ∼1.3% of subjects with European ancestry carry *ACVR1C* LoF variants (10). Additionally, phenome-wide association studies (PheWAS) (12,13) and gene burden tests (https://app.genebass.org/) have not identified any adverse on-target effects associated with ALK7 inhibition.

ALK7 is activated by a subset of TGFβ superfamily ligands, including activins—homodimers of β-subunits encoded by *INHBA*, *INHBB*, *INHBC*, and *INHBE*. Among them, activin B (Act-B) and activin C (Act-C) have been shown to activate ALK7 signaling, but the role of activin E (Act-E) remains unclear (14,15). Activin binding to ALK7 triggers SMAD2/3 phosphorylation, leading to nuclear translocation and regulation of target gene expression. *INHBB* expression is also highest in WAT (https://www.gtexportal.org), suggesting that local Act-B activates ALK7 in this tissue. In contrast, *INHBC* expression is liver-specific. However, the inhibin β C chain (INHBC) circulates in human blood (16–18) and plasma, INHBC levels were shown to be predictive of visceral fat mass (18), and to positively associate with insulin resistance (17), as well as prevalent and incident type 2 diabetes (16,17). INHBC is closely related to INHBE, with 64% amino acid homology (19). *INHBE* is also selectively expressed in hepatocytes and homodimerizes into the orphan ligand Act-E. Rare *INHBE* LoF mutations, like those in *ACVR1C*, are associated with lower WHRadjBMI, lower circulating INHBC levels, and reduced type 2 diabetes and CAD risk (12,13). Global *Inhbe* knockout mice also mirrored the adipose and metabolic phenotypes of global *Acvr1c* knockout mice (20), strongly suggesting that Act-E activates ALK7. Collectively, these data highlight the existence of a potential liver-WAT endocrine axis, governed by Act-C and/or Act-E and ALK7, which regulates fat distribution and systemic metabolism, and appears druggable.

Here, we explored the bidirectional effects between circulating INHBC and adiposity traits, insulin resistance, systemic inflammation, and cardiometabolic disease risk using publicly available genome-wide association study (GWAS) data, several Mendelian randomization (MR) (21,22) approaches (cis-instrument MR [23], polygenic univariable and multivariable MR [MVMR] [24]), and colocalization (25). We hypothesized that liver-derived Act-C promotes upper-body fat distribution, impaired glucose and lipid metabolism, and chronic inflammation via cross talk with ALK7 in WAT.

## RESEARCH DESIGN AND METHODS

A study overview is presented in Supplementary Fig. 1.

### MR

With analogies to randomized controlled trials (Supplementary Fig. 2), we used a drug-target MR framework (Supplementary Fig. 3) to evaluate the cardiometabolic impact of INHBC. As instrumental variables (IVs) for circulating INHBC, we used genome-wide significant ($P < 5E-8$) single nucleotide polymorphisms (SNPs) within 100 kb of the *INHBC* locus (clumped at linkage disequilibrium [LD] $r^2 < 0.2$, genetic distance = 250 kb; 1000 Genomes European reference panel), from a GWAS of plasma INHBC levels measured in 35,559 Icelanders (26). As outcome data, we used the largest publicly available European ancestry GWAS summary statistics for cardiometabolic traits, as well as C-reactive protein (CRP) (a marker of subclinical inflammation), type 2 diabetes, NAFLD, and CAD (Supplementary Tables 1 and 2). To replicate primary findings, we performed additional cis-MRs using fine-mapped IVs identified using Finemap in the PolyFun package (27), as well as cis-protein quantitative trait locus (pQTL) variants extracted from a GWAS of the plasma proteome conducted in the UK Biobank (UKB) (28). To examine reverse causality, we conducted MR studies using exposure instruments extracted from the aforementioned studies ($P < 5E-8$, LD $r^2 < 0.001$, genetic distance = 10 Mb; 1000 Genomes European reference panel), and, as outcome data, GWAS summary statistics for circulating INHBC (26,28).

We used inverse variance weighted (IVW) MR, with MR-Egger regression, MR-Maxlik, and Weighted-Median as sensitivity analyses. For cis-instrument MR analyses, we included a correlation matrix to account for SNP-SNP correlations (29,30). We further conducted MR analyses after excluding variants with larger effects on outcome than the exposure trait (Steiger filtering) (31), as these IVs need not be causal. Where there was evidence of pleiotropy, MR-PRESSO (Mendelian randomization pleiotropy residual sum and outlier) was performed. Results were corrected for multiple comparisons ($P < 0.01$ [0.05/5] based on assessments investigating INHBC and four classes of cardiometabolic traits and subclinical inflammation). For MRs investigating associations between INHBC and the three disease traits, $P < 0.05$ was selected. An IVW $P$ value surpassing multiple testing correction, coupled with directionally consistent associations in all three sensitivity analyses, was considered sufficient evidence to claim a causal effect. For the analysis assessing CRP on INHBC levels, we also

examined the impact of cis-CRP and trans-CRP (removing cis-CRP SNPs) instruments on INHBC.

MVMR analyses were undertaken only if there was evidence for causal effect in the primary MR analyses. All MR and MVMR analyses were conducted using TwoSampleMR (v0.5.7) (32) and MendelianRandomization (v.0.8.0) (29) in *R* (v4.3.1).

### Colocalization

For cis-MR results surpassing multiple comparisons correction, we performed colocalization under the single causal variant assumption, using *coloc* version 5.0.0 (33) to assess whether INHBC shares one or more causal variants with the outcome. We used cis-SNPs (±500 kb) around the *INHBC* locus and considered a posterior probability of >0.7 as evidence that INHBC and the outcome share a causal variant in the *INHBC* locus.

### Phenome-Wide MR

We performed a phenome-wide MR study of 367 diseases and biomarkers (Supplementary Table 3). The outcomes were included if they were performed in cohorts of European ancestry, had ≥1,000 participants, and included at least 100 cases if they were binary variables, and had summary statistics (i.e., β, SEs, effect alleles) for 100,000 SNPs. We performed cis-instrument MR as above and used a Bonferroni corrected *P* value threshold of 1.36E-4 (0.05/367 outcomes).

### Cell Lines

MBdfat5 dedifferentiated fat (DFAT) cell lines (Supplementary Fig. 4) were generated from immortalized human stromovascular cells from a female donor and were cultured, differentiated, and induced to undergo lipolysis as described in Supplementary Methods (34).

We generated the SMAD2/3-luc2-hygro lentiviral reporter construct by cloning the (CAGA)9-MLP sequence (**AGCCAGACAAAAAGCCAGACATTTAGCCAGACA**CTCGAG**AGCCAGACAAAAAGCCAGACATTTAGCCAGACA**CTCGAG**AGCCAGACAAAAAGCCAGACATTTAGCCAGACA**CTCGAGGATATCAAGATCTGGGCTATAAAAGGGGGTGGGGGCGCGTTCGTCCTCACTCTCTTCCA) upstream of the luc2 reporter (Vectorbuilder), and the doxycycline-inducible *ACVR1C* lentivector (pCW-puro-ACVR1C) by cloning the full-length *ACVR1C* open reading frame (NM_145259.3) upstream of an EGFP cassette into the pCW-puro vector (gift from the Broad Institute). Lentiviral particles were packaged in HEK293 cells (CRL-1573; ATCC) using the ViraPower lentiviral packaging mix (#44–2050; Thermofisher Scientific). We generated DFAT[SMAD2/3-luc2] cell lines by SMAD2/3-luc2-hygro lentiviral transduction and selection in 20 μg/mL hygromycin, and cell lines carrying both SMAD2/3-luc2-hygro and pCW-puro-ACVR1C (DFAT[SMAD2/3-luc2/pCW-ACVR1C]) by transducing DFAT[SMAD2/3-luc2] cells with pCW-puro-ACVR1C lenti-particles and selection with 2 μg/mL puromycin.

### Luciferase Assays

DFAT[SMAD2/3-luc2] cells were differentiated in 96-well plates for 12 days, then treated with recombinant human (rh) Act-C (rhAct-C) (1629-AC-010), rhAct-B (659-AB-005; R&D Systems), or vehicle, for ∼24 h. DFAT[SMAD2/3-luc2/pCW-ACVR1C] cells were differentiated for 10 days, then treated with 0.02 or 0.04 μg/mL doxycycline (or vehicle) for 24 h, and a further 24 h with rhAct-C or rhAct-B in addition to doxycycline (or vehicle). Luciferase reporter activity was measured using the Luciferase Assay System (Promega) on a Veritas Microplate Luminometer (Turner Biosystems).

### Western Blotting

DFAT cells were differentiated for 12 days, then treated with 10 ng/mL rhAct-B (or vehicle) for 30 min or with 50 ng/mL rhAct-C (or vehicle) for 1 h. For DFAT[SMAD2/3-luc2/pCW-ACVR1C] cells, on day 10 of differentiation, cells were treated for 2 days with 0.02 μg/mL doxycycline or vehicle, then a further 1 h with 50 ng/mL rhAct-C (or vehicle). Proteins were harvested for Western blotting. Antibodies used were phospho-SMAD2(Ser465/467)/SMAD3(Ser423/425) (D27F4) rabbit mAb and the SMAD2/3 rabbit pAb (#8828 and #5678; Cell Signaling Technology), and horseradish peroxidase–conjugated goat–anti-rabbit secondary antibodies (P0447; DAKO).

### Data and Resource Availability

All MR analyses were conducted using publicly available data, with links to GWAS sources available in Supplementary Table 1, apart from GWAS for BMI-adjusted waist circumference and HCadjBMI. All analyses were completed with existing software packages. Data are available upon request to the corresponding author. Resources are available upon request to the corresponding author.

## RESULTS

### Bidirectional Effects Between Circulating INHBC and Adiposity Traits, Insulin Resistance, and Subclinical Inflammation

We investigated the impact of INHBC on fat distribution, obesity, insulin resistance traits, and subclinical inflammation, using two-sample MR with large GWAS summary data. In univariate IVW MR analyses, higher serum INHBC, measured with an aptamer-based method in 35,559 Icelanders, positively impacted log TAG levels (logTAG) (β ± SE = 0.016 ± 0.002, *P* = 7.37E-26) and had a negative effect on BMI-adjusted hip circumference (HCadjBMI) (β ± SE = −0.027 ± 0.010, *P* = 0.0074) and HDL cholesterol (β ± SE = −0.019 ± 0.002, *P* = 1.33E-18). Positive but weak effects on fasting glucose (β ± SE = 0.006 ± 0.001, *P* = 1.7E-6), LDL cholesterol (β ± SE = 0.008 ± 0.002, *P* = 4.2E-6), and log CRP (logCRP) (β ± SE = 0.007 ± 0.002, *P* = 7.45E-6) were also observed. These results were replicated using INHBC cis-pQTL data derived from an antibody-based plasma proteomic study in 33,687 UKB participants (28). Sensitivity analyses, including

MR-Egger and MR-Maxlik, as well as MR with fine-mapped and Steiger-filtered IVs, confirmed these results with no evidence of directional pleiotropy (Fig. 1*A* and Supplementary Table 4). In summary, circulating INHBC may be causally associated with reduced lower-body fat, dyslipidemia, subclinical inflammation and elevated blood glucose.

To explore whether dysregulated circulating INHBC levels indicate metabolic dysfunction, we conducted reverse univariate MR studies. These showed a negative impact of gluteofemoral adipose tissue (GFAT) volume on plasma INHBC levels (β ± SE = −0.081 ± 0.021, *P* = 1.33E-4). Conversely, WHRadjBMI (β ± SE = 0.103 ± 0.024, *P* = 2.03E-5),

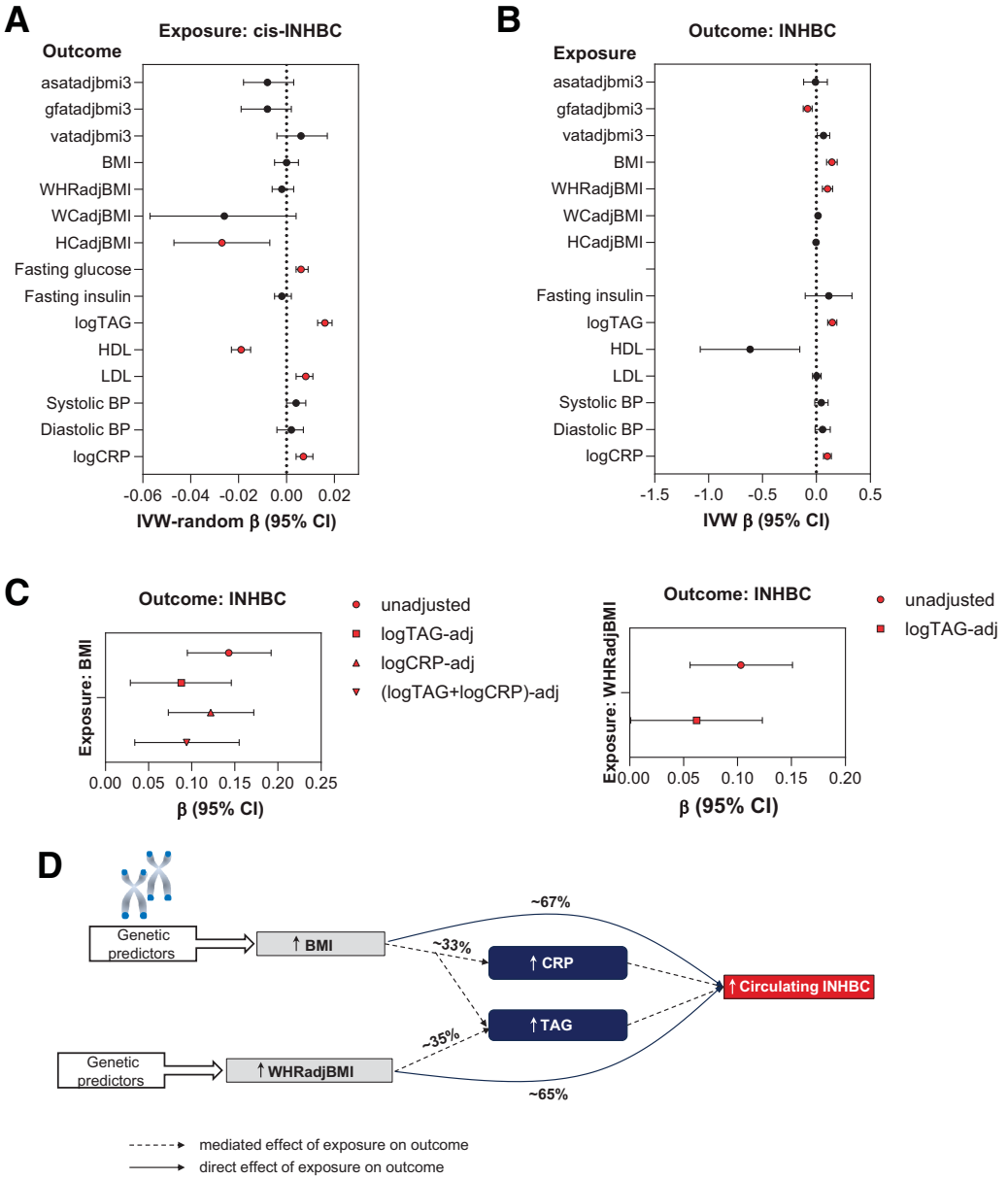


**Figure 1**—Bidirectional MR and multivariable MR investigating the relationship of circulating INHBC (deCODE genetics, Reykjavik, Iceland) with fat distribution, metabolic and blood pressure traits, and systemic inflammation, in sex-combined European populations. *A*: IVW estimates (with 95% CI) from primary cis-MR analyses of the effects of circulating INHBC on anthropometric, blood pressure, and metabolic traits and systemic inflammation (from Supplementary Table 4). *B*: IVW estimates (with 95% CI) of the effects of anthropometric, metabolic and blood pressure traits, and systemic inflammation on circulating INHBC (from Supplementary Table 5). *C*: Mediation analyses: IVW estimates of effects of BMI and WHRadjBMI on circulating INHBC, adjusted for indicated mediator(s) (from Supplementary Table 6). Red-filled symbols denote analyses yielding IVW results with (*A* and *B*) $P < 0.01$ (Bonferroni correction for multiple testing) and that are directionally consistent across all sensitivity analyses, and (*C*) $P < 0.05$ with adjustment for indicated mediator. *D*: Summary for findings of MVMR analyses. asatadjbmi3, BMI and height-adjusted abdominal subcutaneous adipose tissue; gfatadjbmi3, BMI and height-adjusted gluteofemoral adipose tissue; vatadjbmi3, BMI and height-adjusted visceral adipose tissue; WCadjBMI, BMI-adjusted waist circumference.

BMI (β ± SE = 0.143 ± 0.025, $P$ = 6.78E-9), logTAG concentration (β ± SE = 0.147 ± 0.022, $P$ = 1.54E-11), and logCRP levels (β ± SE = 0.102 ± 0.019, $P$ = 4.34E-8) positively affected circulating INHBC. These results were replicated in UKB, where an additional strong positive effect of fasting insulin on circulating INHBC (β ± SE = 0.483 ± 0.171, $P$ = 0.0048) was identified. Sensitivity analyses and Steiger filtering supported these findings (Fig. 1*B* and Supplementary Table 5). While the MR-Egger intercept identified evidence of horizontal pleiotropy for the logTAG effect on INHBC ($P$ = 3.39E-4), removal of pleiotropic variants using MR-PRESSO (Mendelian randomization pleiotropy residual sum and outlier) confirmed the IVW results (β ± SE = 0.157 ± 0.022, $P$ = 1.82E-12). MR analyses using cis and trans logCRP instruments found that the impact of logCRP on INHBC protein levels was not driven by SNPs within the *CRP* locus, supporting that chronic inflammation rather than CRP specifically increases circulating INHBC (cis-CRP $P$ = 0.49, trans-CRP $P$ = 4.95E-7) (Supplementary Table 5).

MVMR analyses revealed that the effect of BMI on circulating INHBC was partially attenuated after adjustment for logTAG and logCRP (Fig. 1*C* and *D* and Supplementary Table 6). Approximately 26% and 23% of the BMI effect on INHBC was mediated by increased circulating TAG and CRP, respectively. Similarly, the effect of WHRadjBMI on INHBC was attenuated by 35% after adjusting for logTAG. These results were replicated in UKB (Supplementary Table 6). In summary, reduced peripheral WAT storage capacity, obesity, hypertriglyceridemia, and chronic inflammation likely lead to higher INHBC levels, with inflammation and elevated TAG levels partially explaining the effects of adiposity traits on circulating INHBC.

### Effects of Circulating INHBC on Type 2 Diabetes, NAFLD, and CAD Risk

Since plasma INHBC levels might constitute both a mediator and a marker of atherogenic dyslipidemia, we investigated the bidirectional effects between INHBC and CAD. Additionally, considering reports that INHBC levels were positively associated with prevalent and incident type 2 diabetes (16,17), and that hepatic *INHBE* expression is upregulated in subjects with hepatosteatosis (13), we examined the bidirectional effects between INHBC and type 2 diabetes and NAFLD. Univariate IVW MR revealed that higher circulating INHBC slightly increased the risk of CAD (odds ratio [OR] = 1.021, 95% CI = 1.008–1.034) and NAFLD (OR = 1.006, 95% CI = 1.002–1.011). Furthermore, type 2 diabetes positively impacted INHBC levels (β = 0.074, SE = 0.010, $P$ = 6.01E-13), while CAD had a negative effect (β = −0.029, SE = 0.013, $P$ = 0.026). These results were replicated with fine-mapped INHBC IVs and pQTL data from UKB, and were directionally consistent in sensitivity analyses and robust to Steiger filtering (Fig. 2 and Supplementary Tables 7 and 8). MVMR analyses showed that 40% of the effect of INHBC on CAD risk was mediated by changes in TAG and HDL and LDL cholesterol levels (Supplementary Table 9). Conversely, the impact of type 2 diabetes on plasma INHBC levels persisted after adjusting for logTAG, suggesting independence from type 2 diabetes–associated hypertriglyceridemia. In summary, INHBC might be causally associated with slightly higher CAD and NAFLD risk, and its levels are increased in type 2 diabetes. An atherogenic lipid profile may partially explain the effects of INHBC on CAD risk.

### Colocalization Analyses

To address the possibility that distinct causal variants influence circulating INHBC levels and metabolic traits or disease outcomes because of LD (22), we conducted colocalization studies (Supplementary Table 10). INHBC showed strong evidence of colocalization with lipid traits, fasting glucose, logCRP, and CAD (posterior probability of hypothesis 4 [PP.H4] > 0.7). These results were replicated in UKB (Supplementary Table 10). The credible set overlap was resolved to two variants within the *INHBC* gene: rs2229357, a missense variant ($INHBC_{R322Q}$) predicted to be damaging by two out of six bioinformatic tools, and rs3741414, a 3′ UTR variant (Supplementary Table 11). These data further support the causal link between INHBC and these phenotypes.

### MR PheWAS Highlights INHBC as a Novel Drug Target for Hyperlipidemia and Cardiometabolic Disorders

To explore potential on-target effects of pharmacologic INHBC inhibition, we explored the impact of circulating INHBC on 367 traits (Supplementary Table 3) using cis-MR (Fig. 3 and Supplementary Table 12). INHBC had a positive impact on the risk of familial combined hyperlipidemia (OR = 1.032, 95% CI = 1.018–1.047), hypercholesterolemia (OR = 1.002, 95% CI = 1.001–1.003), and statin use (OR = 1.018, 95% CI = 1.011–1.026). Moreover, higher plasma INHBC levels were linked with higher risk of hyperuricemia (β ± SE = 0.025 ± 0.003, $P$ = 2.15E-21), gout (OR = 1.002, 95% CI = 1.001–1.002), and impaired renal function, as determined by estimated glomerular filtration rate (β ± SE = −0.002 ± 0.000, $P$ = 8.06E-23), serum urea (β ± SE = 0.014 ± 0.002, $P$ = 3.91E-11), and serum creatinine levels (β ± SE = 0.010 ± 0.001, $P$ = 1.24E-16), although the effect sizes were small. INHBC was also causally associated with lower aspartate transaminase (AST) levels (β ± SE = −0.015 ± 0.003, $P$ = 4.21E-8) and higher calcium levels (β ± SE = 0.008 ± 0.002, $P$ = 1.08E-3). These findings were replicated in UKB (Supplementary Table 13) and confirmed by Steiger-filtered and reverse MR analyses (Supplementary Tables 14 and 15). Colocalization analyses indicated shared causal variants between INHBC levels and all aforementioned traits (all posterior probabilities of hypothesis 4 [PP.H4] > 0.88), except for AST, and calcium levels (Supplementary Table 10). Consistent with primary outcomes, rs2229357 and rs3741414 were identified as credible set variants (Supplementary Table 11). These results reinforce our primary findings and suggest that pharmacologic inhibition of INHBC might protect against gout and renal failure.

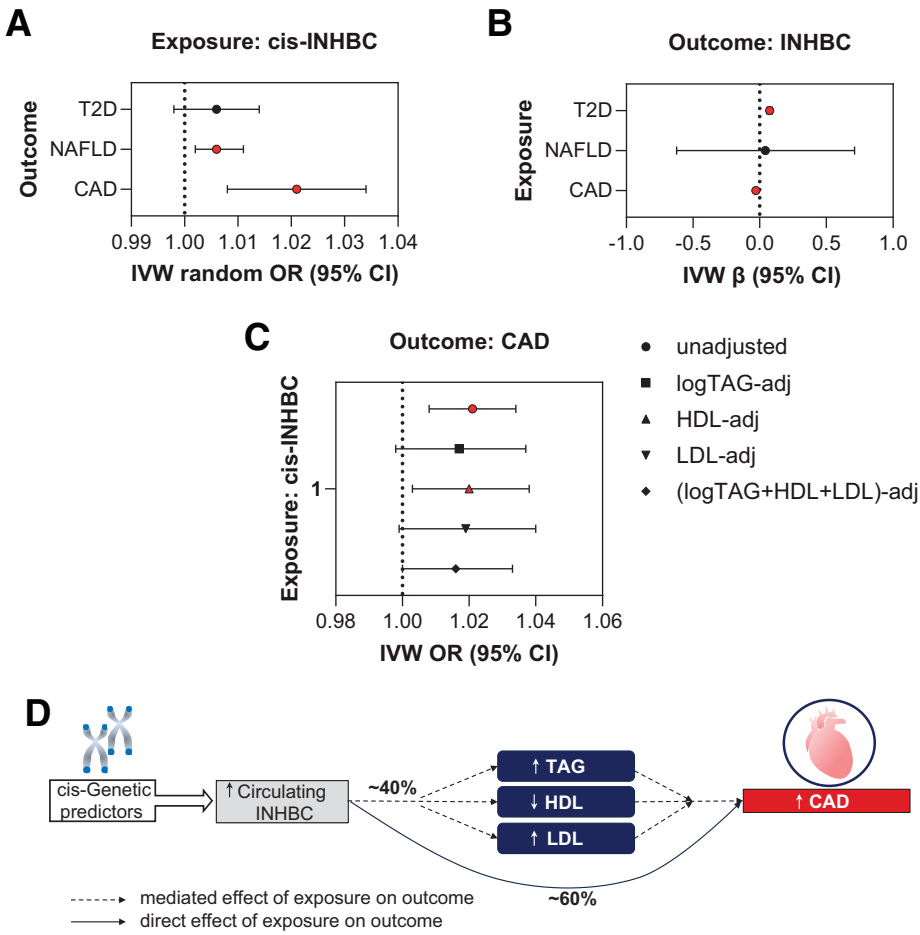


**Figure 2**—Bidirectional MR and multivariable MR investigating the relationship of circulating INHBC (deCODE genetics, Reykjavik, Iceland) with type 2 diabetes (T2D), NAFLD, and CAD in sex-combined European populations. *A*: IVW estimates (OR with 95% CI) from primary cis-MR analyses of the effects of circulating INHBC on T2D, NAFLD, and CAD (from Supplementary Table 7). *B*: IVW estimates (with 95% CI) of the effects of T2D, NAFLD, and CAD on circulating INHBC (from Supplementary Table 8). *C*: Mediation analyses: IVW estimates of effects of INHBC on CAD (sex-combined), adjusted for indicated mediator(s) (from Supplementary Table 9). *D*: Summary for findings of MVMR analyses. Red-filled symbols denote analyses yielding IVW results with (*A* and *B*) $P < 0.05$ and that are directionally consistent across all sensitivity analyses, and (*C*) $P < 0.05$ with adjustment for indicated mediator.

### Activin C Functions as an ALK7 Ligand in Human Adipocytes

Previous research showed that Act-C acts as an ALK7 ligand capable of inducing SMAD2 phosphorylation in differentiated mouse adipocytes (15). In the same experiments, Act-C treatment throughout differentiation reduced adipocyte lipid accumulation. Considering these results and the inverse association of INHBC with gluteofemoral adiposity, we investigated the impact of rhAct-C on SMAD2/3 signaling in immortalized human abdominal and gluteal DFAT adipocytes. Unlike rhAct-B, rhAct-C only very weakly stimulated SMAD2/3 phosphorylation and promoter reporter activity in these cells (Fig. 4*A* and *B*). Given the significantly lower expression of *ACVR1C* in in vitro differentiated abdominal and gluteal adipocytes compared with primary adipocytes (Fig. 4*C*), we also tested rhAct-C in DFAT cells transduced with a doxycycline-inducible ACVR1C vector. Treatment with 0.02 µg/mL doxycycline for 48 h resulted in approximately four- and twofold increase in *ACVR1C* expression in abdominal and gluteal DFAT adipocytes, respectively, compared with vehicle-treated cells, reaching around twofold higher levels than endogenous *ACVR1C* in primary abdominal adipocytes and equivalent levels in gluteal adipocytes (Fig. 4*C*). In these transduced cells, rhAct-C evidently stimulated promoter reporter activity and SMAD2/3 phosphorylation (Fig. 4*D–F*). rhAct-C was approximately half as potent as rhAct-B in activating SMA2/3 signaling (Supplementary Fig. 5). Finally, rhAct-C suppressed adrenaline-stimulated lipolysis without affecting adipogenesis (Fig. 4*G* and *H*). These findings confirm Act-C as an ALK7 ligand and lend support to the existence of endocrine cross talk between liver-derived Act-C and WAT ALK7.

## DISCUSSION

We investigated the bidirectional effects between circulating INHBC and adiposity traits, insulin resistance, chronic

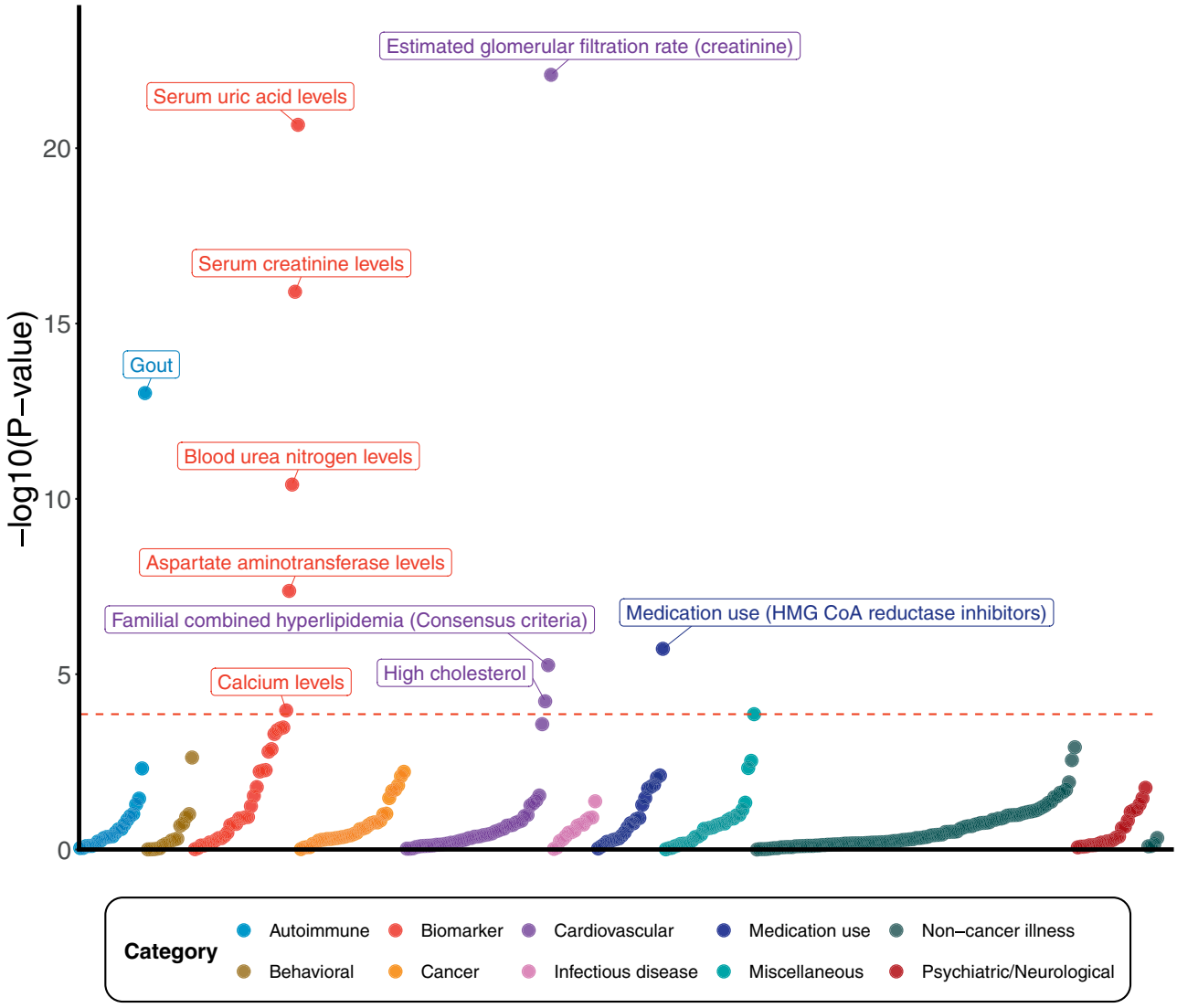


**Figure 3**—Phenome-wide Mendelian randomization of circulating INHBC protein levels (deCODE genetics, Reykjavik, Iceland). Results of drug-target MR screen of INHBC protein levels on 367 traits across 11 categories. The *y* axis is the −log10(*P* value) of the inverse variance weighted MR estimates, and labeled outcomes surpassed Bonferroni correction for multiple comparisons (*P* value = 1.36E-4 [0.05/367 outcomes]). See also Supplementary Table 12.

inflammation, and cardiometabolic disease risk. Our findings show causal relationships between higher plasma INHBC levels and reduced lower-body fat and atherogenic dyslipidemia, and slightly increased systemic inflammation and blood glucose levels. Higher plasma INHBC also increased the risk of CAD and NAFLD, although the latter association was not supported by colocalization analyses. Additionally, circulating INHBC levels were upregulated consequent to obesity, lower peripheral WAT storage capacity, hypertriglyceridemia, inflammation, and type 2 diabetes. These results suggest a potential vicious cycle whereby elevated INHBC contributes to dyslipidemia and systemic inflammation, further increasing INHBC levels. This cycle likely exacerbates cardiovascular disease risk in individuals with obesity, upper-body fat distribution, and type 2 diabetes. Finally, our data align with and extend the findings of previous studies linking raised circulating INHBC levels with prevalent and incident type 2 diabetes (16,17).

Mechanistically, the link between higher plasma INHBC levels and CAD is partly mediated by dyslipidemia. INHBC was causally associated with only a slight increase in the risk of CAD and NAFLD, with each 1-SD increase in INHBC raising CAD and NAFLD risk by approximately 2.1% and 0.6%, respectively. However, MR analyses using UKB INHBC pQTL data indicated higher ORs of about 5.6% and 1.5%, respectively. Secondly, if the liver is a primary site of INHBC action, ORs based on circulating INHBC levels might underestimate its impact on NAFLD risk. Thirdly, using the same pQTL data set as for INHBC (26), plasma ANGPTL3 levels, an established drug target for atherogenic dyslipidemia (35), did not affect the risk of CAD (OR = 1.006, 95% CI = 0.965–1.049), NAFLD (OR = 0.974, 95% CI = 0.947–1.002),

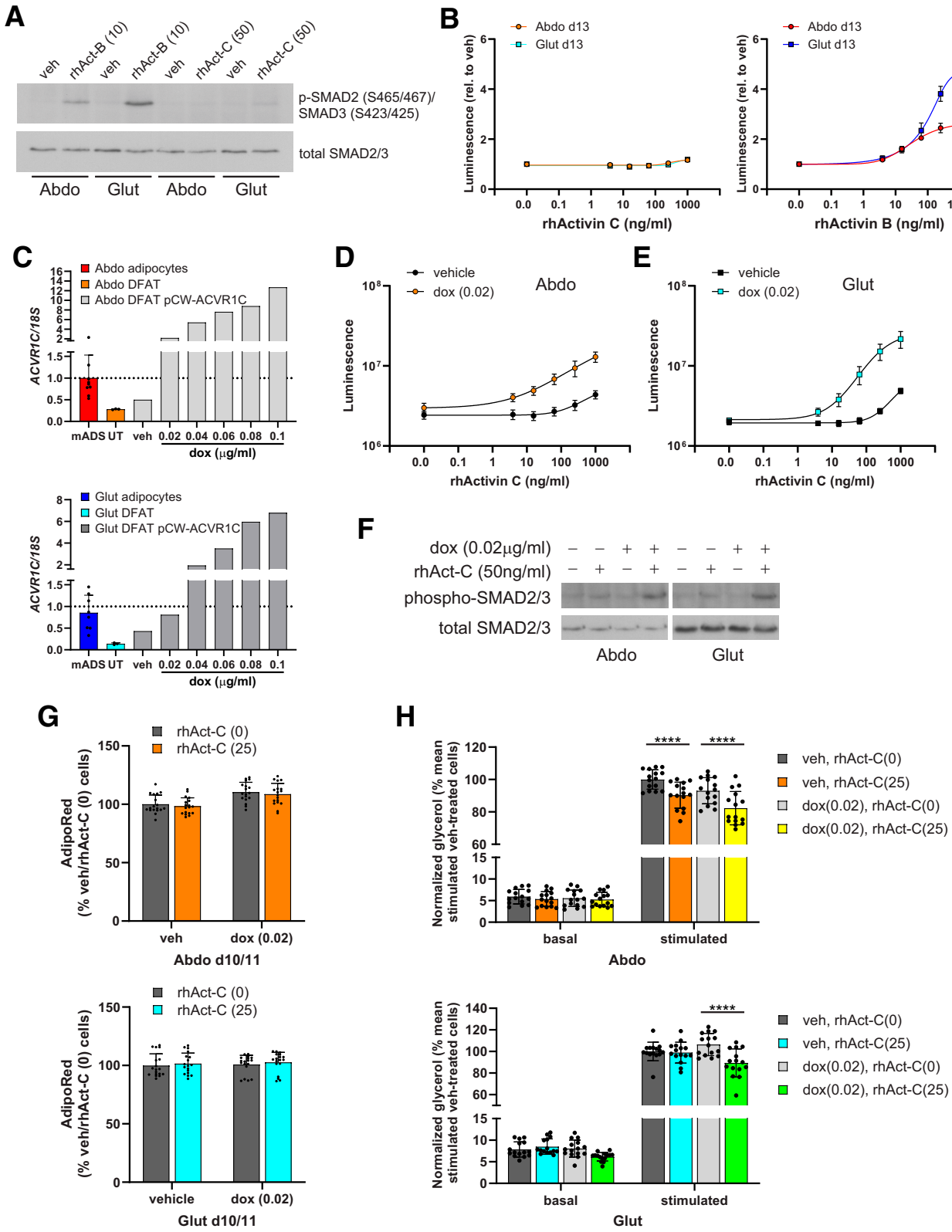


**Figure 4—**Activin-C is an ALK7 ligand. *A*: Western blots of phospho-SMAD2/3 and total SMAD2/3 in 12-day in vitro differentiated abdominal and gluteal DFAT cells after 30-min and 1-h treatment with rhAct-B (10 ng/mL) and rhAct-C (50 ng/mL), respectively, or vehicle (veh). *B*: SMAD2/3 luciferase-reporter assay in in vitro differentiated DFAT cells following 24-h treatment with rhAct-C ($n$ = 4) and rhAct-B ($n$ = 8). Data are means ± SD. *C*: Comparison of *ACVR1C* expression in isolated mature adipocytes (from $n$ = 8–9 female donors), 14-day in vitro differentiated untransduced (UT) DFAT cells, and 12-day in vitro differentiated DFAT[SMAD2/3-luc2/pCW-ACVR1C] cells treated with increasing doses of doxycycline for 24 h. qPCR results are normalized to *18S*. Dotted line indicates mean *ACVR1C* expression level in abdominal mature adipocytes. *D* and *E*: SMAD2/3-luciferase reporter assay in DFAT adipocytes coexpressing a dox-inducible ACVR1C

or type 2 diabetes (OR = 0.996, 95% CI = 0.945–1.050). Similarly, circulating levels of FGF21, an established drug target for NAFLD (36), had no impact on NAFLD (OR = 0.98, 95% CI = 0.95–1.01) or CAD (OR = 0.99, 95% CI = 0.93–1.05) risk, and were causally associated with increased type 2 diabetes risk (OR = 1.11, 95% CI = 1.03–1.20). Fourthly, the ORION-3 trial demonstrated that administering inclisiran, a siRNA targeting hepatic *PCSK9* mRNA, twice yearly achieved a 62–78% average reduction in circulating PCSK9 levels over 4 years (37). Since *PCSK9* is not exclusively expressed in the liver (https://www.gtexportal.org), a similar approach might produce more significant reductions in plasma INHBC levels. Thus, targeting INHBC with monoclonal antibodies or siRNAs could serve as an effective adjunct treatment of combined hyperlipidemia, CAD, and, potentially, NAFLD. Finally, we show that the effects of adiposity traits on plasma INHBC levels are partly mediated by circulating TAG and chronic inflammation. In contrast, hypertriglyceridemia did not account for the link between type 2 diabetes and higher circulating INHBC, which could be mediated by hyperinsulinemia instead.

Our MR PheWAS results offer additional support that inhibiting INHBC could alleviate dyslipidemia. Additionally, INHBC-targeting drugs might protect renal function and reduce gout risk, although the impact of circulating INHBC on these traits was small. The MR PheWAS also suggested that INHBC inhibition might be associated with slightly higher AST and calcium levels. However, colocalization analyses did not support these findings, and INHBC was not associated with higher risk of cirrhosis (Supplementary Tables 10, 12, and 13). Furthermore, homozygous global *Inhbc* knockout mice did not display overt phenotypic differences from wild-type mice (38). Further preclinical studies are needed to explore the efficacy and side effect profile of INHBC inhibitors in treating dyslipidemia and cardiometabolic disorders.

Our in vitro experiments confirm that Act-C acts as an ALK7 ligand in human adipocytes, consistent with findings in mouse WAT-derived adipocytes (15). In immortalized adipocytes overexpressing *ACVR1C* to levels similar to those in primary abdominal and gluteal adipocytes, rhAct-C stimulated SMAD2/3 phosphorylation and promoter reporter activity, although less potently than rhAct-B. In the same experiments, while rhAct-C had no effects on adipogenesis, it suppressed adrenaline-stimulated lipolysis. Consistent with these findings, circulating INHBC levels negatively impacted HCadjBMI, possibly because lipolysis serves to generate ligands for PPARγ and RXRα, key adipogenic transcription factors (39,40). Although we did not find significant associations between INHBC and MRI-derived fat distribution measures, this may be due to the limited power from the small sample size of UKB participants with MRI scans.

In contrast to *INHBC*, a rare, *INHBE* LoF variant (rs150777893) was associated with lower WHRadjBMI at GWAS significance (12,13). *INHBE* was also robustly linked with WHRadjBMI based on rare variant burden tests (12) (https://t2d.hugeamp.org/gene.html?gene=INHBE). Additionally, animal studies strongly suggest that Act-E acts as an endocrine ligand for ALK7 in WAT. Specifically, *Inhbe* knockout mice exhibited enhanced WAT lipolysis and resistance to high-fat diet–induced obesity, similar to global *Acvr1c* knockout animals (20). Directly opposite phenotypes were observed in mice with hepatic overexpression of *Inhbe*, which were abrogated in animals with concomitant *Acvr1c* knockout (20). Collectively, these findings, along with our data, suggest that WAT-derived Act-B and liver-derived Act-E primarily activate ALK7 in WAT. However, rhAct-E is not currently commercially available, and no studies have measured circulating INHBE or Act-E levels in humans. Nonetheless, ectopically expressed *INHBE* was secreted from CHO and HEK293T cells, while secretion of the rs150777893 mutant was markedly impaired (12,13). Based on our findings and previous research (15), we also speculate that Act-C may influence systemic metabolism through endocrine actions in WAT, potentially suppressing lipid turnover similar to Act-E. Act-C and Act-E might also impact hepatic lipid and glucose metabolism, since *ACVR1C* is also expressed in the liver, albeit at lower levels than in WAT, and ALK7 protein has been detected (https://www.proteinatlas.org). Further research, including metabolic phenotyping of *Inhbc*-knockout mice (38), is needed to confirm these hypotheses.

Activins are homodimers of two inhibin β-chains. In addition to homodimers, several heterodimers, namely Act-AB and Act-AC, have been detected. Inhibin β-chains can also form heterodimers with inhibin α-chains, encoded by *INHA*, to produce inhibins that antagonize activins. Our study concentrated on circulating INHBC levels, which may not directly reflect plasma levels of Act-C. However, the formation of mature heterodimers necessitates coexpression of both β-chains or both α- and β-chains in the same cell. Hepatic expression of *INHA* (0.9 transcripts per million [nTPM]), *INHBA* (9.2 nTPM) and *INHBB* (19.6 nTPM) are substantially lower than

vector. Day 10 abdominal (*D*) and gluteal (*E*) adipocytes were treated with 0.02 μg/mL doxycycline (or vehicle) for 24 h, then a further 24 h with addition of increasing doses of rhAct-C ($n = 12$, from three independent experiments). Data points are means ± SD relative luminescence units. *F*: Western blots of phospho-SMAD2/3 and total SMAD2/3 in 12-day in vitro differentiated DFAT[SMAD2/3-luc2/pCW-ACVR1C] adipocytes, cultured for ∼48 h in the presence of 0.02 μg/mL doxycycline or vehicle prior to a 1-h treatment with rhAct-C (50 ng/mL) or vehicle. *G*: Effects of rhAct-C (25 ng/mL) treatment of DFAT[SMAD2/3-luc2/pCW-ACVR1C] on adipogenesis ($n = 12$ from three independent experiments). Cells were treated throughout differentiation. *H*: Effects of rhAct-C (25 ng/mL) treatment on lipolysis ($n = 15$, from five independent experiments). In vitro differentiated day 10 cells were cultured in the presence of 0.02 μg/mL doxycycline or vehicle for 24–48 h, then a further ∼24 h with the addition of 25 ng/mL rhAct-C or vehicle, prior to the lipolysis experiments. Histograms are means ± SD. Statistical tests: (*G*) two-way ANOVA with Tukey multiple comparisons test; (*H*) three-way ANOVA with Sidak multiple comparisons test. ****$P < 0.0001$.

that of *INHBC* (159 nTPM) and *INHBE* (144 nTPM) (https://www.proteinatlas.org). Therefore, the majority of circulating INHBC is likely in the form of Act-C or Act-CE, assuming INHBC and INHBE can heterodimerize.

There are limitations to the cis-instrument MR framework. First, cis-instrument MR estimates do not reflect side effects or other physiological responses related to specific drug classes (23). Additionally, as MR estimates reflect lifelong modulation of the target, caution is necessary in interpreting both the therapeutic and side effect profiles for shorter duration pharmacologic modulation (23). Second, assessing violations of MR assumptions, such as horizontal pleiotropy, is challenging (21); however, we included several complementary MR methods, each accommodating orthogonal assumptions about genetic pleiotropy (32), and found broadly consistent results across all analyses strengthening causal inference (21). Further, while cis-instrument MR is less susceptible to horizontal pleiotropy and heterogeneity than conventional two-sample MR (23), there is still the potential for pleiotropy or heterogeneity. Importantly, we found strong evidence of a shared causal variant in the *INHBC* locus between INHBC protein levels and many of the significant outcomes in the drug-target MR analysis, which, when combined with the drug-target MR findings, suggest common biological pathways and mechanisms linking INHBC and these outcomes. The pQTL and outcome data sets used in this study are derived from participants of European ancestry, limiting the generalizability of these findings to other populations. Finally, clear Act-C activity was observed only in in vitro differentiated human adipocytes when *ACVR1C* was overexpressed, even though the levels of *ACVR1C* mRNA achieved through overexpression were similar to those found in primary adipocytes. Consequently, these results should be interpreted with caution.

In summary, we identify INHBC as a promising therapeutic target for atherogenic dyslipidemia, and potentially CAD and NAFLD, with possible additional benefits for improving renal function and reducing gout risk. Our data suggest that INHBC influences systemic metabolism through both local and endocrine effects on ALK7 in the liver and WAT, respectively. Further research is needed to establish the therapeutic benefits and side effect profile of INHBC inhibition, as well as to elucidate the cellular and molecular mechanisms underlying its effects on systemic metabolism.

**Acknowledgments.** The authors thank Xue Lu Wang and Amy Barrett, Oxford Centre for Diabetes, Endocrinology and Metabolism, University of Oxford, for generating the pCW-puro-ACVR1C construct and for assistance with glycerol measurements, respectively, and acknowledge the participants and investigators of the studies used in this research without whom this effort would not have been possible.

**Funding.** This work was funded by British Heart Foundation Clinical Research Fellowships to C.C. (FS/16/45/32359 and FS/SCRF/24/32029).

**Duality of Interest.** No potential conflicts of interest relevant to this article were reported.

**Author Contributions.** N.Y.L. and D.B.R. researched data, contributed to discussion, and wrote, reviewed, and edited the manuscript. R.R. and R.N. generated GWAS data. G.D.S., D.R., F.K., and F.W.L. reviewed and edited the manuscript. C.C. conceptualized, wrote, reviewed, and edited the manuscript and obtained funding. C.C. is the guarantor of this work and, as such, had full access to all the data in the study and takes responsibility for the integrity of the data and the accuracy of the data analysis.

## References

1. Danforth E Jr. Failure of adipocyte differentiation causes type II diabetes mellitus? Nat Genet 2000;26:13
2. Virtue S, Vidal-Puig A. Adipose tissue expandability, lipotoxicity and the metabolic syndrome–an allostatic perspective. Biochim Biophys Acta 2010;1801:338–349
3. Abifadel M, Varret M, Rabès J-P, et al. Mutations in PCSK9 cause autosomal dominant hypercholesterolemia. Nat Genet 2003;34:154–156
4. Cohen JC, Boerwinkle E, Mosley TH, Hobbs HH. Sequence variations in PCSK9, low LDL, and protection against coronary heart disease. N Engl J Med 2006;354:1264–1272
5. Sabatine MS, Giugliano RP, Keech AC, et al.; FOURIER Steering Committee and Investigators. Evolocumab and clinical outcomes in patients with cardiovascular disease. N Engl J Med 2017;376:1713–1722
6. Zamani N, Brown CW. Emerging roles for the transforming growth factor-β superfamily in regulating adiposity and energy expenditure. Endocr Rev 2011;32:387–403
7. Lee M-J. Transforming growth factor beta superfamily regulation of adipose tissue biology in obesity. Biochim Biophys Acta Mol Basis Dis 2018;1864:1160–1171
8. Dani C. Activins in adipogenesis and obesity. Int J Obes (Lond) 2013;37:163–166
9. Ibáñez CF. Regulation of metabolic homeostasis by the TGF-β superfamily receptor ALK7. Febs J 2022;289:5776–5797
10. Emdin CA, Khera AV, Aragam K, et al. DNA sequence variation in ACVR1C encoding the activin receptor-like kinase 7 influences body fat distribution and protects against type 2 diabetes. Diabetes 2019;68:226–234
11. Koprulu M, Zhao Y, Wheeler E, et al. Identification of rare loss-of-function genetic variation regulating body fat distribution. J Clin Endocrinol Metab 2022;107:1065–1077
12. Deaton AM, Dubey A, Ward LD, et al.; AMP-T2D-GENES Consortium. Rare loss of function variants in the hepatokine gene INHBE protect from abdominal obesity. Nat Commun 2022;13:4319
13. Akbari P, Sosina OA, Bovijn J, et al.; DiscovEHR Collaboration. Multiancestry exome sequencing reveals INHBE mutations associated with favorable fat distribution and protection from diabetes. Nat Commun 2022;13:4844
14. Tsuchida K, Nakatani M, Yamakawa N, Hashimoto O, Hasegawa Y, Sugino H. Activin isoforms signal through type I receptor serine/threonine kinase ALK7. Mol Cell Endocrinol 2004;220:59–65
15. Goebel EJ, Ongaro L, Kappes EC, et al. The orphan ligand, activin C, signals through activin receptor-like kinase 7. Elife 2022;11:e78197
16. Gudmundsdottir V, Zaghlool SB, Emilsson V, et al. Circulating protein signatures and causal candidates for type 2 diabetes. Diabetes 2020;69:1843–1853
17. Cronjé HT, Mi MY, Austin TR, et al. Plasma proteomic risk markers of incident type 2 diabetes reflect physiologically distinct components of glucose-insulin homeostasis. Diabetes 2023;72:666–673
18. Williams SA, Kivimaki M, Langenberg C, et al. Plasma protein patterns as comprehensive indicators of health. Nat Med 2019;25:1851–1857
19. Hashimoto O, Tsuchida K, Ushiro Y, et al. cDNA cloning and expression of human activin betaE subunit. Mol Cell Endocrinol 2002;194:117–122
20. Adam RC, Pryce DS, Lee JS, et al. Activin E-ACVR1C cross talk controls energy storage via suppression of adipose lipolysis in mice. Proc Natl Acad Sci U S A 2023;120:e2309967120
21. Sanderson E, Glymour MM, Holmes MV, et al. Mendelian randomization. Nat Rev Methods Primers 2022;2:6

22. Hemani G, Bowden J, Davey Smith G. Evaluating the potential role of pleiotropy in Mendelian randomization studies. Hum Mol Genet 2018;27:R195–R208
23. Schmidt AF, Finan C, Gordillo-Marañón M, et al. Genetic drug target validation using Mendelian randomisation. Nat Commun 2020;11:3255–3255
24. Sanderson E, Davey Smith G, Windmeijer F, Bowden J. An examination of multivariable Mendelian randomization in the single-sample and two-sample summary data settings. Int J Epidemiol 2018;48:713–727
25. Giambartolomei C, Vukcevic D, Schadt EE, et al. Bayesian test for colocalisation between pairs of genetic association studies using summary statistics. PLoS Genet 2014;10:e1004383
26. Ferkingstad E, Sulem P, Atlason BA, et al. Large-scale integration of the plasma proteome with genetics and disease. Nat Genet 2021;53:1712–1721
27. Weissbrod O, Hormozdiari F, Benner C, et al. Functionally informed fine-mapping and polygenic localization of complex trait heritability. Nat Genet 2020;52:1355–1363
28. Sun BB, Chiou J, Traylor M, et al.; Regeneron Genetics Center. Plasma proteomic associations with genetics and health in the UK Biobank. Nature 2023;622:329–338
29. Yavorska OO, Burgess S. MendelianRandomization: an R package for performing Mendelian randomization analyses using summarized data. Int J Epidemiol 2017;46:1734–1739
30. Henry A, Gordillo-Marañón M, Finan C, et al.; HERMES and SCALLOP Consortia. Therapeutic targets for heart failure identified using proteomics and Mendelian randomization. Circulation 2022;145:1205–1217
31. Hemani G, Tilling K, Davey Smith G. Orienting the causal relationship between imprecisely measured traits using GWAS summary data. PLoS Genet 2017;13:e1007081
32. Hemani G, Zheng J, Elsworth B, et al. The MR-Base platform supports systematic causal inference across the human phenome. Elife 2018;7:e34408
33. Tissink E, Werme J, de Lange SC, et al. The genetic architectures of functional and structural connectivity properties within cerebral resting-state networks. eneuro 2023;10:ENEURO.0242-0222.2023
34. Loh NY, Minchin JEN, Pinnick KE, et al. RSPO3 impacts body fat distribution and regulates adipose cell biology in vitro. Nat Commun 2020;11:2797
35. Markham A. Evinacumab: first approval. Drugs 2021;81:1101–1105
36. Loomba R, Sanyal AJ, Kowdley KV, et al. Randomized, controlled trial of the FGF21 analogue pegozafermin in NASH. N Engl J Med 2023;389:998–1008
37. Ray KK, Troquay RPT, Visseren FLJ, et al. Long-term efficacy and safety of inclisiran in patients with high cardiovascular risk and elevated LDL cholesterol (ORION-3): results from the 4-year open-label extension of the ORION-1 trial. Lancet Diabetes Endocrinol 2023;11:109–119
38. Lau AL, Kumar TR, Nishimori K, Bonadio J, Matzuk MM. Activin βC and βE genes are not essential for mouse liver growth, differentiation, and regeneration. Mol Cell Biol 2000;20:6127–6137
39. Schreiber R, Hofer P, Taschler U, et al. Hypophagia and metabolic adaptations in mice with defective ATGL-mediated lipolysis cause resistance to HFD-induced obesity. Proc Natl Acad Sci U S A 2015;112:13850–13855
40. Ström K, Gundersen TE, Hansson O, et al. Hormone-sensitive lipase (HSL) is also a retinyl ester hydrolase: evidence from mice lacking HSL. FASEB J 2009;23:2307–2316